Available online at www.sciencedirect.com
SCIENCE DIRECT®

Journal of the European Ceramic Society 23 (2003) 1705–1713
www.elsevier.com/locate/jeurceramsoc

Thermal crystallization of ion-exchanged zeolite A

M.C. Mascolo, G. Dell'Agli, C. Ferone, M. Pansini, G. Mascolo*

Laboratorio Materiali del Dipartimento di Meccanica, Strutture, Ambiente e Territorio, Facoltà di Ingegneria di Cassino, Via G. di Biasio 43, 03043 Cassino (FR), Italy

Received 1 March 2002; received in revised form 14 October 2002; accepted 20 October 2002

Abstract

The zeolite 4A ($Na_{12}Al_{12}Si_{12}O_{48}\cdot 27H_2O$) was subjected to cationic exchange with an aqueous solution of Li^+ 0.5 M at 70 °C. After three exchanges for 24 h, about 100% of Na^+ was removed obtaining the Li-exchanged form (Li)-A. Despite this quite complete exchange, some undesired and occluded $NaAlO_2$ was detected in the typical structural cages of precursor. The partial exchange of Li with equivalent amounts of Ca or Mg, allowed the formation of (Li–Ca)- or (Li–Mg)-exchanged zeolitic forms characterized by different Ca or Mg contents, respectively. These various zeolitic precursors have been thermally treated at increasing temperatures up to 1170 °C. The transformations into other crystalline phases occur immediately after the formation of intermediate amorphous phases originating from the thermal collapse of zeolitic precursors. From the (Li)-A zeolite-based precursor, a small amount of nepheline ($NaAlSiO_4$) and β-eucryptite ($LiAlSiO_4$) crystallize, while during the thermal transformation of Li–Ca-containing precursors, anorthite [$(Ca,Na)Al_2Si_2O_8$] and β-eucryptite-like phase are formed. Stuffed derivatives of quartz relatively richer in SiO_2 crystallize from (Li–Mg)-containing precursors. The Mg content of the zeolitic precursor affects the type of secondary crystallized phases and consequently the composition of the corresponding stuffed derivative of quartz.
© 2003 Elsevier Science Ltd. All rights reserved.

Keywords: Anorthite; Crystallization; Eucryptite; Nepheline; Phase development; Zeolite; Zeolitic precursors

1. Introduction

Beta-eucryptite ($LiAlSiO_4$) is an end-member of the solid solution series between $LiAlSiO_4$ and SiO_2 which are called stuffed derivatives of high-quartz structure.[1–3] It has a low density (2.36 g/cm^3) and a negative thermal linear coefficient of expansion (-0.34×10^{-6}/°C in the range 20–700 °C).[4–7] It incongruently melts at ~1400 °C[8] and on cooling it crystallizes into the monoclinic stuffed high quartz structure.[9] Glass-ceramic materials belonging to the Li_2O–Al_2O_3–$nSiO_2$ system, with $n=2$ to 10, are characterised by low-expansion coefficients and are used in applications where dimensional stability during temperature fluctuations is critical.[10] Unlike solid solutions of β-spodumene glass-ceramics, where $n=4$ to 10, β-eucryptite glass-ceramics with $n=2$ exhibit poor mechanical strength. The decreased strength in these materials is due to micro-stresses at the interface between the residual glass matrix and crystallized phases during the controlled crystallization of the glassy precursor. Micro-stressing occurs because of the different expansion coefficients of the residual glass and the crystalline phase. Further stresses are caused by high thermal expansion anisotropy of β-eucryptite-based crystal especially during the cooling of polycrystalline material from the sintering temperature. Both features produce microcracks and extensive fracturing of the material that result in poor mechanical properties.

A large number of aluminosilicate zeolites may be employed as precursors to obtain ceramic products.[11–20] By changing the Si/Al ratio of the zeolitic frameworks and the different types of nonframework cations it is possible to obtain raw materials with components mixed at atomic level. Since zeolites have a very low framework density, as compared to analogous nonzeolitic compositions, all aluminosilicate zeolites transform at increasing temperatures into denser products. On the other hand, metastable thermal transformation products may be obtained which are impossible to obtain with traditional synthesis techniques.[19] The thermal collapse of the less dense zeolitic framework can directly produce other crystalline phases or intermediate amorphous

* Corresponding author. Tel.: +39-0776-299710; fax: +39-0776-299711.
E-mail address: mascolo@unicas.it (G. Mascolo).

0955-2219/02/$ - see front matter © 2003 Elsevier Science Ltd. All rights reserved.
PII: S0955-2219(02)00418-1

phases before crystallization. In the latter case, a controlled crystallization of intermediates can be performed as that of base glasses in the manufacturing of glass-ceramics.

The numerous advantages of glass-ceramics, as compared to ceramics, are well known. However, after thermal treatment, glass-ceramics consist of a varying crystalline phases and a residual glass matrix.

The present study was undertaken to investigate the thermal transformations of Li-exchanged zeolite 4A as a precursor of β-eucryptite, as the dehydrated zeolite exactly reproduces the $LiAlSiO_4$ composition. In particular, the goal is to ascertain the presence of residual amorphous phases after thermal crystallization as it occurs in devitrified glass-ceramics. In addition, the effects of partial Li substitution with equivalent Mg or Ca contents will be examined emphasizing the eventual formation of microcracks due to the formation of microstresses as generally results for β-eucryptite-based ceramics.

2. Experimental

Synthetic zeolite 4A ($Na_{12}Al_{12}Si_{12}\cdot 27H_2O$), (R.G. of C. Erba, Italy) was used in this investigation. The zeolite powder was cation-exchanged to replace Na^+ with Li^+. This powder will hereafter be referred to as (Li)-A sample. In this case the cation exchange was performed as follows: 100 g of zeolite 4A was contacted for 24 h with 3.0 L of Li^+ 0.50 M solution at 70 °C with continuous stirring. The solid was separated from the liquid through filtration and again contacted with a new solution of Li^+ 0.50 M for a total of three times. The resulting (Li)-A powder was washed with distilled water, dried at 60 °C, and finally allowed to reached equilibrium at room temperature and relative humidity of about 50%.

Further and partial substitutions of different Li content of (Li)-A sample with Mg and Ca, respectively, were performed through cation exchange with Mg- and Ca-containing solutions as follows: four different solutions, displaying different Mg^{2+} and Ca^{2+} concentrations, respectively, were prepared. Each solution was contacted with 20 g of (Li)-A powder for 3 h under stirring in order to obtain four zeolite samples characterized by a partial and different substitution of Li^+ with equivalent content of Mg^{2+} and Ca^{2+}, respectively. These powders will hereafter be referred to as L, H(Li–Mg)-A and L, H(Li–Ca)-A samples, respectively, where the letters L, and H refer, respectively, to a low and high equivalent fraction of Mg or Ca replacing Li.

The cation compositions of the resulting zeolitic precursors were characterized by measuring the cation concentration of the solutions obtained dissolving each zeolite sample in a hydrofluoric and perchloric acid solution. The concentrations of Li, Na, Mg and Ca were determined by atomic absorption spectrophotometry, using a Perkin-Elmer Analyst 100 apparatus.

The samples thermally untreated and 2-h thermally treated at increasing temperatures were also characterized by X-ray diffraction analysis (XRD), using a Philips X'PERT diffractometer and CuK_α radiation.

Table 1
Li, Na, Mg and Ca equivalent fractions of different zeolite samples

Zeolite	Li	Na[a]	Mg	Ca
(Li)-A	0.98	0.02	–	–
L(Li–Mg)-A	0.95	0.02	0.03	–
H(Li–Mg)-A	0.86	0.02	0.12	–
L(Li–Ca)-A	0.94	0.02	–	0.04
H(Li–Ca)-A	0.82	0.02	–	0.16

[a] 0.12 meq/g of Na as occluded $NaAlO_2$.

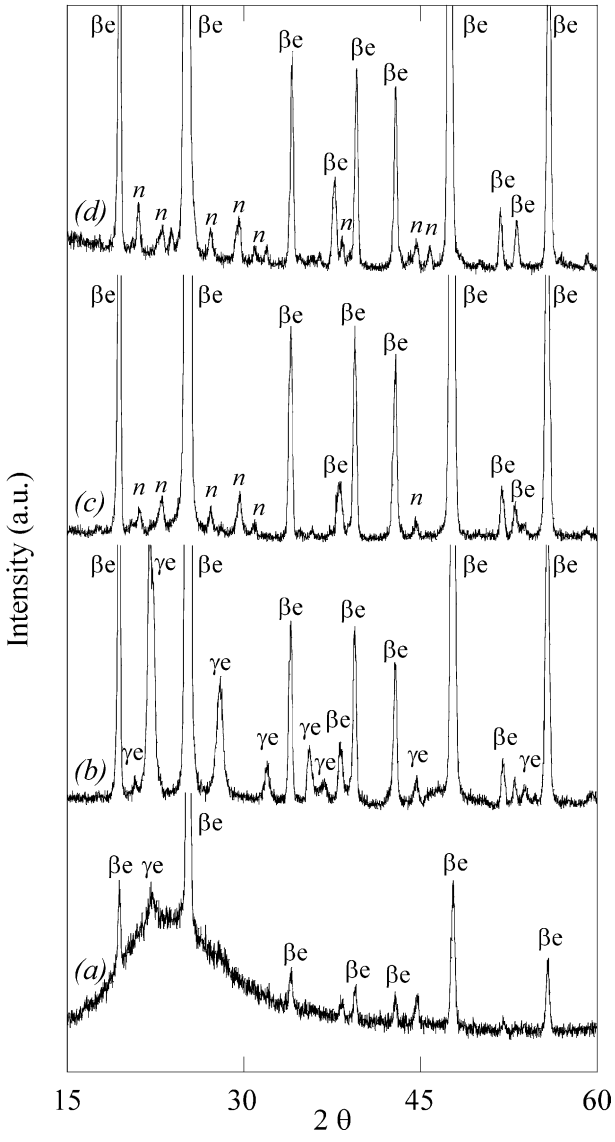

Fig. 1. XRD patterns of (Li)-A precursor after thermal treatments for 2 h at 700 °C (a), 750 °C (b), 900 °C (c) and 1170 °C (d). βe = β-eucryptite; γe = γ-eucryptite; *n* = nepheline.

Simultaneous differential thermal analysis (DTA) and thermogravimetric analysis (TGA) were made using a Netzsch thermoanalyzer model STA 409, using α-Al_2O_3 as reference and a heating rate of 10 °C/min.

The thermodilatometric analysis was performed in air on green pellet 10 mm high and with 10 mm diameter, obtained by isostatically pressing powders at 150 MPa.

A surface of the sintered products was polished with 1 μm diamond, chemically etched in 2% HF solution for 15 s, and observed by scanning electron microscopy (SEM) using a Philips model XL30.

3. Results and discussion

3.1. Cation composition of the zeolite samples

The chemical compositions of various cations, in terms of equivalent fraction, present in the zeolite samples are given in Table 1. Some unchanged Na content (0.02 meq/g) is still present in (Li)-A sample and in the remaining four samples characterised by a low and high Ca or Mg content, respectively. It must be taken into account that in all the samples there is an additional and unchangeable Na content present as occluded $NaAlO_2$ in the typical cages of the starting zeolitic structure corresponding to a Na content of 0.12 meq/g.

3.2. X-ray diffraction

3.2.1. (Li)-A sample

XRD patterns of the (Li)-A sample heated with a ramp of 10 °C/min and 2-h thermally treated at increasing temperatures are reported in Fig. 1. The zeolitic precursor still persists as a crystalline phase up to 675 °C, while at 700 °C a large amount of amorphous phase is present, some β-eucryptite of the poor silica variety[21] and traces of both the zeolite precursor and γ-eucryptite also called zeolite A(BW),Li.[20,22] The thermally treated samples at 720, 750 and 800 °C are mostly made up by β-eucryptite, γ-eucryptite and traces of a residual amorphous phase. At the higher temperatures of the thermal treatment, i.e. 850, 900, 1000 and 1170 °C, γ-eucryptite and the amorphous phase are practically absent, and some nepheline ($NaAlSiO_4$)[23] appears together with the β-eucryptite as the main crystalline phase.

To measure semiquantitatively the amount of β-eucryptite at increasing temperatures of the thermal treatment, the intensity of the strongest peak $(\bar{1}12)$ of β-eucryptite (see Fig. 1a) was measured for each XRD pattern. A speedy increase of β-eucryptite content occurs at 730 °C, followed by a further but more moderate increase up to 1170 °C (Fig. 2).

Apart from the presence of some undesired amounts of both Na (0.14 meq/g) and Al (0.12 meq/g as $NaAlO_2$), the composition of the dehydrated zeolitic precursor corresponds exactly to that of $LiAlSiO_4$. Taking also into account that the nepheline crystallized as the secondary phase, that it displays the same Al/Si ratio of the zeolitic precursor, and the absence of residual amorphous phase, the composition of the main crystallized phase must correspond to that of β-eucryptite, i.e. the end member in the solid solutions of $LiAlSiO_4$–SiO_2 system. No significant change in the *d* spacings for the X-ray reflections of β-eucryptite was observed, in fact, for the whole temperature range of thermal treatment, in contrast with the high-quartz solid solutions thermally crystallized from glasses having the same composition.[24] Traces of Li-spinel and residual uncrystallized glass were, in fact, detected as secondary phases involving a crystallization of β-eucryptite richer in SiO_2.

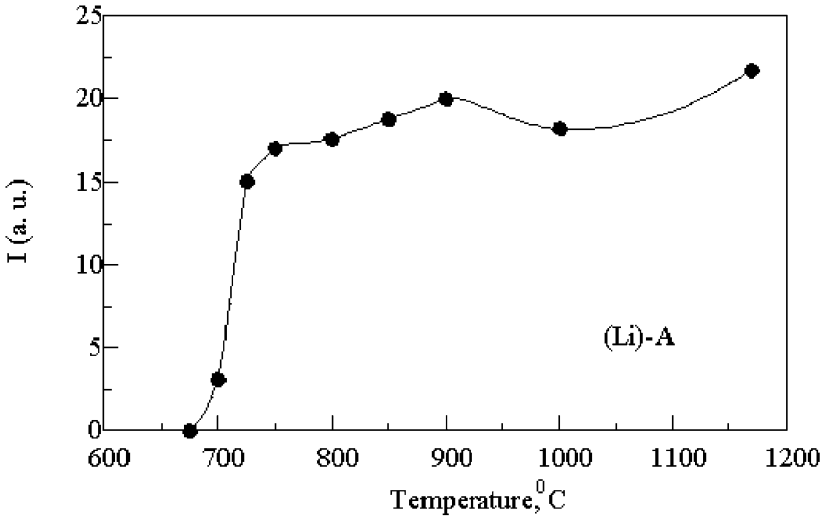

Fig. 2. β-eucryptite content in (Li)-A precursor thermally treated for 2 h at increasing temperature up to 1170 °C.

3.2.2. (Li-Ca)-A samples

The thermal crystallization of the two (Li–Ca)-A-based precursors was performed in the same conditions as for the (Li)-A sample. For sake of brevity only the XRD patterns of L(Li–Ca)-A sample are reported (Fig. 3). At 700 °C, the zeolitic precursor still persists in spite of the formation of a certain amount of the amorphous phase. At 725, 750 and 800 °C, the continuous diminution of the amorphous phase content is in correspondence with the rapid increase of both β-eucryptite-like phase and γ-eucryptite contents. At 850 °C, an amorphous phase is still present, while γ-eucryptite disappears, and some nepheline crystallizes. At higher temperatures of thermal treatment, i.e. at 900, 1000 and 1170 °C, the result is a continuous crystallization of anorthite $(Ca,Na)Al_2Si_2O_8$,[25] with traces of nepheline and with β-eucryptite-like phase as the main crystallized phase.

The thermal treatments performed on H(Li–Ca)-A sample, give the same crystalline phases. The main difference between the two samples of the (Li–Ca)-A series concerns the content of crystallized anorthite the amount of which increases with the increase of the Ca content of the zeolite precursor. A further difference concerns the temperature of the corresponding transformations; i.e. the higher the Ca content of the zeolitic precursor, the higher the temperature of crystallization. No significant change in the *d* spacings for the X-ray reflections of β-eucryptite was observed, neither at different temperature of thermal treatment nor for the different Ca content of the precursors. These findings demonstrate that the main crystallized phase for the (Li–Ca)-A series is very close to that of β-eucryptite. Likewise the behaviour detected for the (Li)-A sample, the two precursors of (Li–Ca)-A series also show a initial speed increase of β-eucryptite-like phase content at approximately 750 (Fig. 4) °C followed by a further but more moderate increase up to 1170 °C.

3.2.3. (Li–Mg)-A samples

The thermal crystallizing behaviour of the two (Li–Mg)-A samples is also affected by the Mg content of the zeolitic precursor. After the treatment at 700 °C, the sample with the lowest Mg content (L(Li–Mg)-A) shows a small collapse (Fig. 5), while between 725 and 850 °C, after the structural collapse, a decreasing amount of amorphous phase and a corresponding increase of a β-eucryptite-like phase content results. Between 900 and 1000 °C, some mullite ($3Al_2O_3{\cdot}2SiO_2$) and traces of nepheline crystallize, while at 1170 °C, mullite disappears and corundum (α-Al_2O_3) and a spinel-like phase ($MgO{\cdot}Al_2O_3$) result. The secondary phases detected either at intermediate temperatures or at 1170 °C, involve a variable composition for the main β-eucryptite-like phase. In the presence of mullite, the composition of β-eucryptite-like phase must be richer in SiO_2 and contains the starting Mg according to previous findings.[24] At higher temperatures of thermal treatment, the reduced solubility of Mg in β-eucryptite-like phase determines an exsolution of Mg with formation of spinel. The displacement of the overlapped XRD

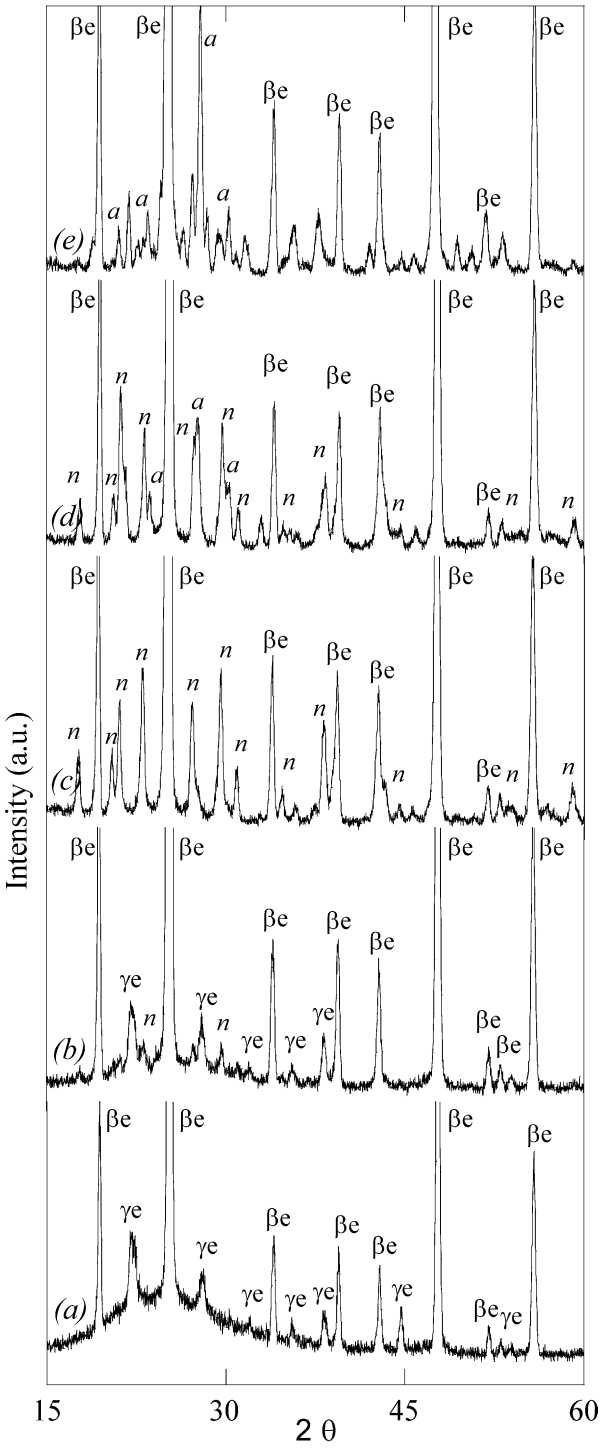

Fig. 3. XRD patterns of L(Li–Ca)-A precursor after thermal treatments for 2 h at 725 °C (a), 800 °C (b), 850 °C (c), 900 °C (d) and 1170 °C (e). βe = β-eucryptite-like phase; γe = γ-eucryptite; *n* = nepheline; *a* = anorthite.

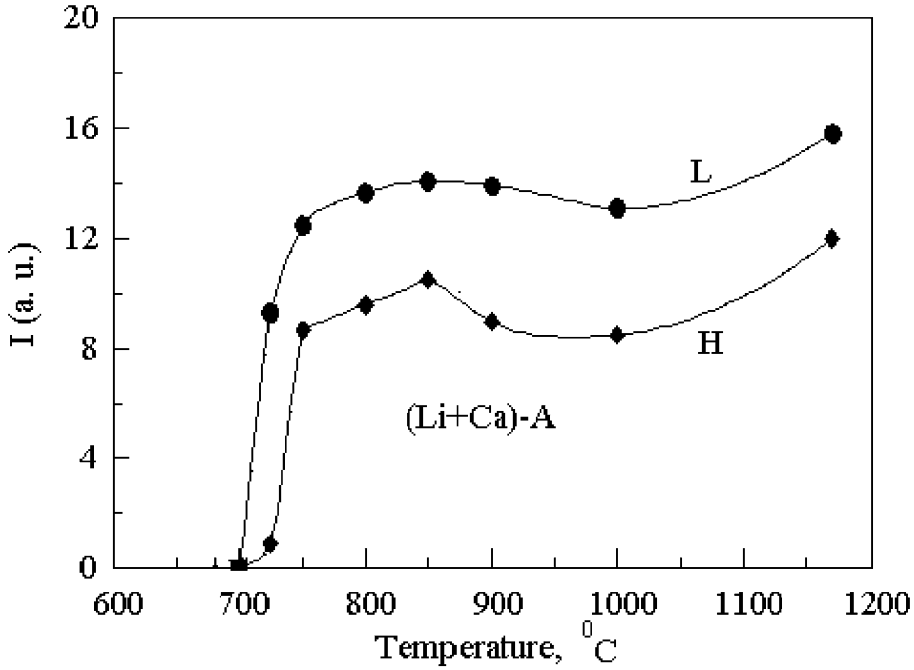

Fig. 4. β-eucryptite-like phase contents in L(Li–Ca)-A and H(Li–Ca)-A precursors thermally treated for 2 h at increasing temperature up to 1170 °C.

$(\bar{1}1\bar{4})$, $(1\bar{2}4)$ and $(2\bar{1}\bar{4})$ reflections of β-eucryptite-like phase at increasing temperatures of thermal treatment in Fig. 6, confirms, in fact, the changeable composition of such phase.

From the not reported XRD patterns of thermally treated H(Li–Mg)-A sample, the following transformations have been noticed. At 700 °C, the zeolitic precursor is practically collapsed, traces of precursor, β-eucryptite-like phase and γ-eucryptite are also present, while an increased amount of β-eucryptite-like phase results at 725 °C. Between 800 and 1000 °C, nepheline and β-eucryptite-like phase result. Finally spinel also crystallizes at 1170 °C. The main differences among these precursors concern the amount of crystallized spinel-like phase detected at 1170 °C. The higher the Mg content of the starting precursor, the higher the content of crystallized spinel-like phase (Fig. 7) and consequently a β-eucryptite richer in SiO_2 results. On the other hand, the spinels obtained from different Mg-containing precursors also show different compositions. The higher the Mg content of starting precursor, the higher the Mg content of the corresponding spinel as appears by comparing the displacements of XRD reflections of spinels crystallized from the two corresponding precursors (Fig. 7). It is well known that extensive substitutional solid solutions occur between the stoichiometric $MgO{\cdot}Al_2O_3$ and γ-Al_2O_3,[26] and a displacement at lower diffraction angles involves a spinel richer in MgO, as can be detected for the spinel crystallized from the H(Li–Mg)-A precursor characterized by the highest Mg content (Fig. 7). Hence, the lower the Mg content of the precursor, the more a spinel richer in Al_2O_3 crystallizes. In the last case, the formation of α-Al_2O_3 at 1170 °C involves that at temperatures lower than 1170 °C, a spinel richer in Al_2O_3 content crystallizes from which exolves α-Al_2O_3 at higher temperature of thermal treatment.

The amount of β-eucryptite-like phase detected by XRD analysis at increasing temperatures of thermal treatment of the (Li–Mg)-A series shows a maximum at an intermediate temperature of the thermal treatment. This result demonstrates that at intermediate temperatures the incorporation of Mg in the β-eucryptite-like phase still persists, while at higher temperatures secondary crystalline phases originate from such a phase with a consequent decrease of its content.

3.3. Thermal analysis and thermodilatometry

The DTA curves of Li–A sample and (Li–Ca)-A series are reported in Fig. 8. The very large endothermic peak at low temperature is due to the progressive dehydration of all the zeolite samples. More interesting appear the exothermic effects at higher temperature attributable to the crystallization effects. The (Li)-A sample shows two close and sharp exothermic peaks at 745 and 775 °C followed by a small exothermic one at 893 °C (Fig. 9a). The L(Li–Ca)-A sample having the lowest Ca content, also shows two sharp exothermic peaks at 757 and 800 °C followed by a small broad one at 880 °C. For the H(Li:=Ca)-A sample, analogous peaks are shifted at higher temperatures, i.e. 764, 811 and 917 °C, respectively.

It is difficult to explain the two close exothermic peaks detected for all the samples. In this case the crystallization

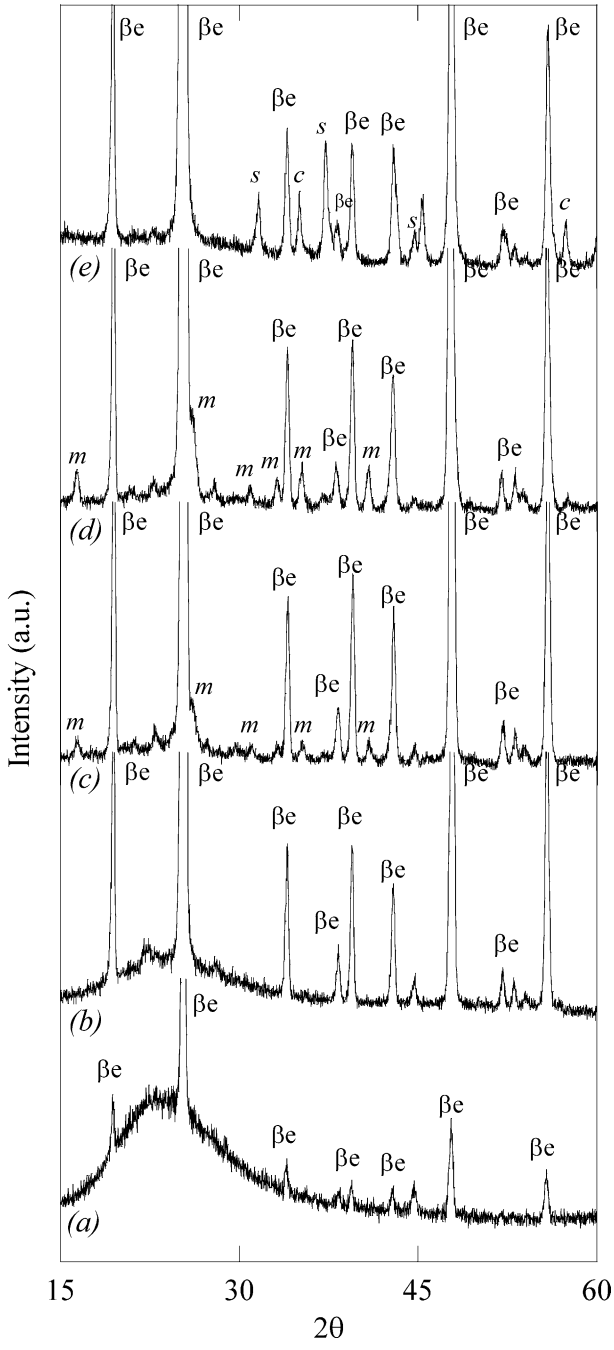

Fig. 5. XRD patterns of L(Li–Mg)-A precursor after thermal treatments for 2 h at 725 °C (a), 750 °C (b), 900 °C (c), 1000 °C (d) and 1170 °C (e). βe = β-eucryptite-like phase; *m* = mullite; *s* = spinel; *c* = corundum.

of the various precursors takes place immediately after their full structural collapse. For an analogous sample of zeolite A containing both Na and Li, the thermal collapse precedes the formation of crystalline phases,[19] whereas for the pure zeolite Li-A(BW) the amorphous phase was not observed during the thermal treatment.[20] On the other hand, the polymorph γ-eucryptite was found to crystallize from the isostructural Li-A(BW) which in turn transforms into β-eucryptite.[20] Such a

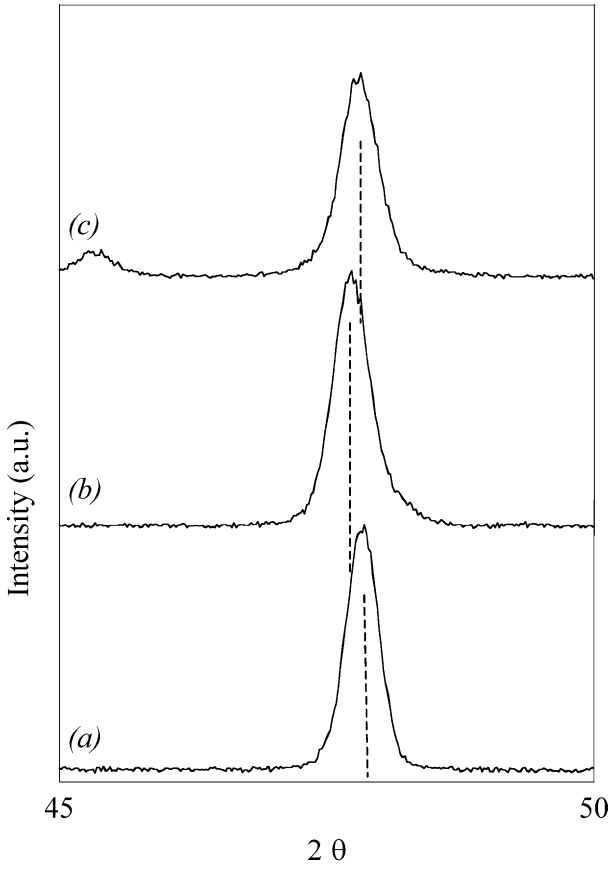

Fig. 6. Displacement of overlapped XRD $(\bar{1}\bar{1}4)$, $(1\bar{2}4)$ and $(2\bar{1}4)$ reflections of β-eucryptite-like phase recorded for L(Li–Mg)-A precursor after 2 h of thermal treatment at increasing temperature.

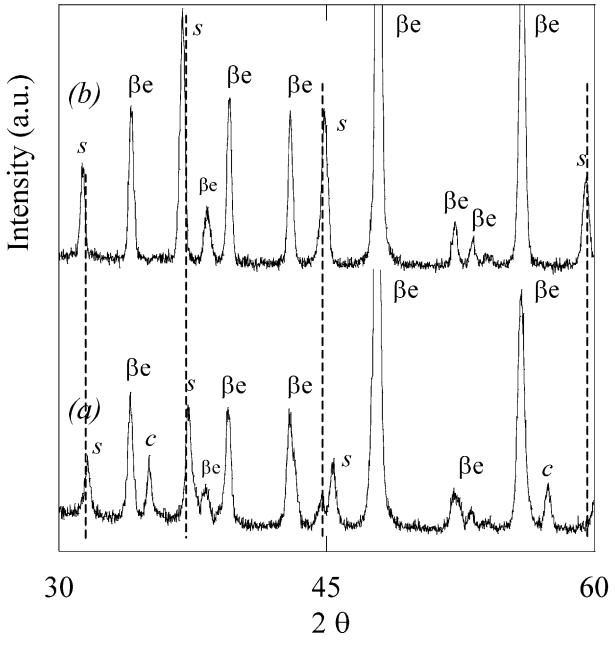

Fig. 7. XRD patterns of L(Li–Mg)-A and H(Li–Mg)-A samples thermally treated for 2 h at 1170 °C. βe = β-eucryptite-like phase; *s* = spinel; *c* = corundum. Note the displacement of XRD peaks of spinel crystallized from the two precursors.

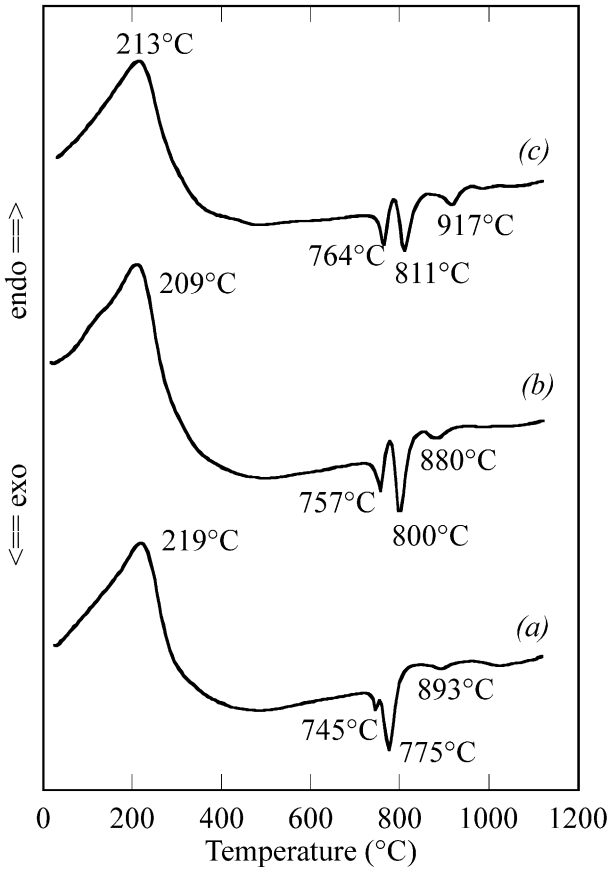

Fig. 8. DTA curves of (Li)-A (*a*), L(Li–Ca)-A (*b*) and H(Li–Ca)-A (*c*) precursors.

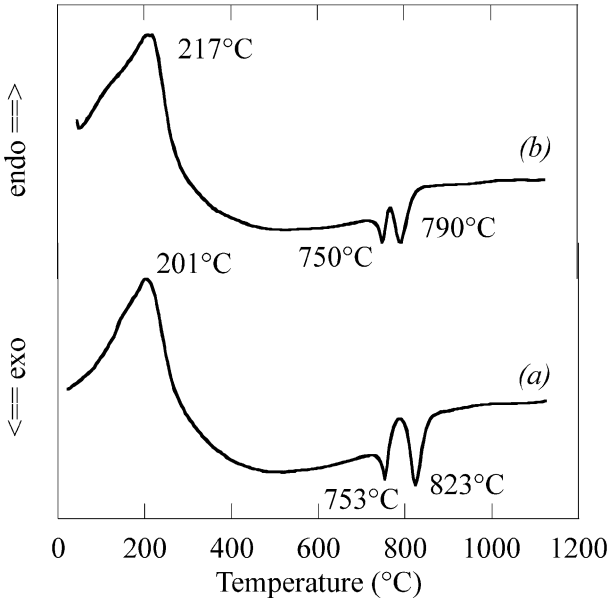

Fig. 9. DTA curves of L(Li–Mg)-A and H(Li–Mg)-A samples, respectively.

transformation is characterized by a sharp endotermic peak at ~1000 °C. As the thermal behaviour of the (Li)-A precursor resembles that of Li-A(BW), several concomitant thermal transformations must be considered with the two mentioned close exothermic effects: the collapse of the zeolitic precursor, the crystallization of γ-eucryptite, and finally the transformation of γ-eucryptite into β-eycryptite. As the structural collapse of zeolite precursor takes place in a wide range of temperature, no sharp DTA signal is to be expected. On the other hand, a lower temperature for the γ-eucryptite → β-eucryptite transformation is to be expected for the impure (Li)-A sample due to the presence of some Na content. It can be deduced the two close exothermic peaks are the resulting signals of the exothermic peak of crystallization of γ-eucryptite and the endothermic peak due to the transformation of γ-eucryptite into β-eucryptite. The small exothermic effect at 893 °C, detected for the (Li)-A precursor, has been attributed to nepheline crystallization, while the analogous effects at 880 and 917 °C, present in L(Li–Ca)-A and H(Li–Ca)-A samples, respectively, have been attributed to the anorthite crystallization.

The thermal behaviour of the two (Li–Mg)-A samples is characterized by the presence of two exothermic signals (Fig. 9). The H(Li-Mg)-A sample shows these peaks at 750 and 790 °C, whereas for L(Li–Mg)-A the peaks shift to 753 and 823 °C, respectively.

For the sake of brevity only the thermodilatometric curve of (Li)-A sample as a green pellet has been reported in Fig. 10. A small shrinkage in the temperature range 200–400 °C, followed by a strong shrinkage around 750 °C, and finally a further strong shrinkage at temperatures higher than 1100 °C have been detected. The shrinkage at low temperature and the strong shrinkage at 750 °C have been attributed to a typical effect of dehydration and the thermal collapse of the zeolite structure,[27] respectively, while the strong shrinkage at temperature

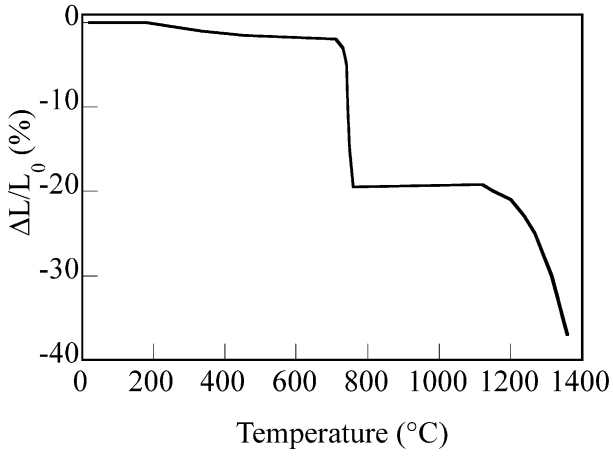

Fig. 10. Thermodilatometric curve of (Li)-A precursor as powdered compact isostatically cold pressed at 150 MPa.

higher than 1100 °C is due to the sintering effect of the compact.

Cylindrical compacts of the samples listed in Table 1, isostatically pressed at 150 MPa, have been sintered at 1170 °C for 2 h and slowly cooled. The thermal cycle adopted for all the samples has been performed as follows: a first ramp with a heating rate of 5 °C/min was adopted in the temperature range 25–350 °C, followed by a ramp with a heating rate of 20 °C/min up to 700 °C, then another ramp with heating rate of 5 °C/min in the temperature range 700–900 °C, followed by the final ramp with a heating rate of 20 °C/min up to 1170 °C. After a 2 h hold at 1170 °C, the sintered compacts have been slowly cooled with a cooling rate of 2 °C/min.

3.4. Microstructure analysis

The SEM surface morphology of the sintered (Li)-A sample, previously polished and etched with a solution containing 2.0% HF for 15 s, is presented in the micrography of Fig. 11a. A polycrystalline and porous microstructure with an extensive formation of microcracks can be observed. In this circumstance, the microstresses are not caused by the difference in the thermal linear coefficients of expansion between the residual glass and crystalline phases as it happens for analogous glass precursors. Instead the microstresses develop mainly from the high thermal expansion anisotropy of β-eucryptite, as the zeolitic precursor is fully crystallized. The micrography of Fig. 11b, which refers to the L(Li–Ca)-A sample, presents a polycrystalline and less porous microstructure with the presence, also in this case, of a certain amount of microcracking. Moreover, it can be observed that the secondary anorthite preferentially crystallizes at the boundaries between the bigger sized crystals of β-eucryptite-like phase. H(Li–Ca)-A sample (Fig. 11c) is similar to that observed for the L(Li-Ca)-A sample. It displays a less dense matrix, less numerous microcracks and an highest content of anorthite as a secondary phase. H(Li–Mg)-A sample displays a microstructure with rare microcracks (Fig. 11d). Such finding can be related to the formation of a β-eucryptite-like phase richer in SiO_2 which is characterized by a reduced thermal expansion anisotropy.[6] The micrography shows also very small crystals of spinel ($MgOAl_2O_3$) more frequent in the zeolitic precursor characterized by the highest Mg content.

4. Conclusions

Zeolitic precursors based on Li-exchanged zeolite A and on (Li–Ca)- and (Li–Mg)-exchanged zeolite A, require a relatively high temperature of thermal treatment for the full structural collapse to proceed into an amorphous phase. The partial substitution of Li^+ with

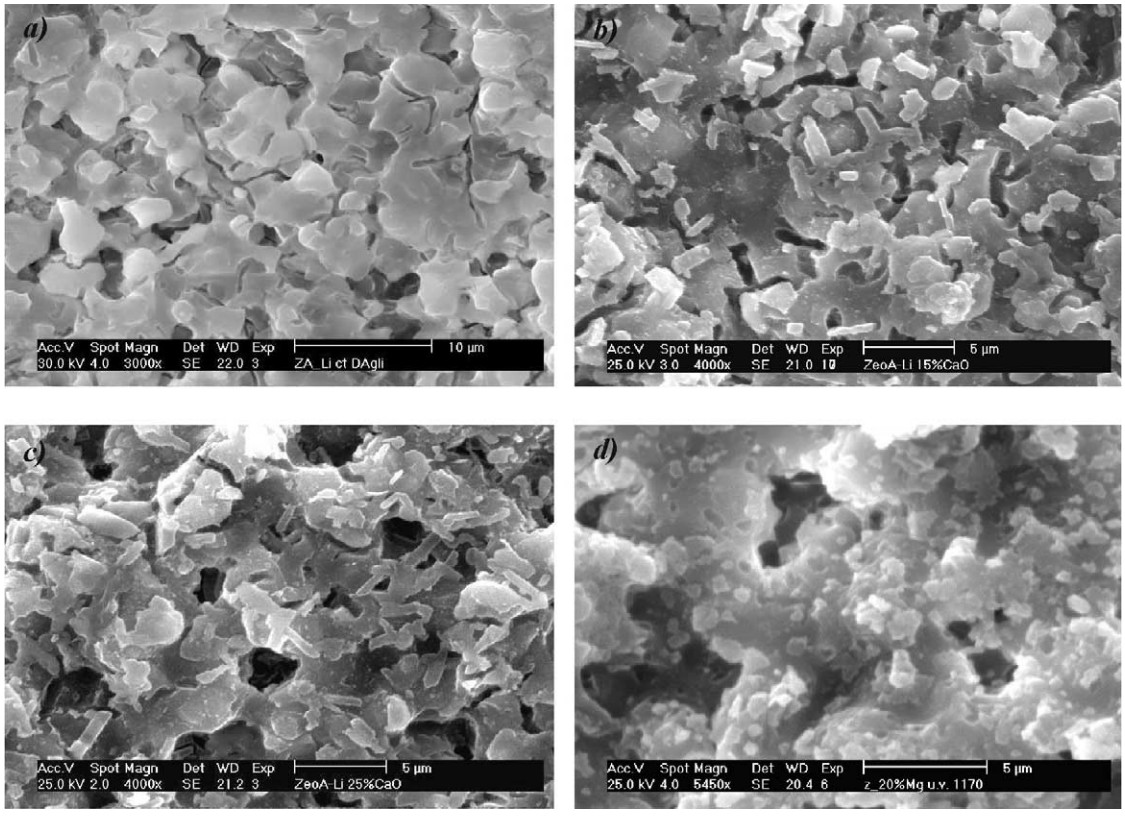

Fig. 11. SEM micrographs of (Li)-A (a), L(Li–Ca)-A (b), H(Li–Ca)-A (c) and H(Li–Mg)-A (d) precursors sintered at 1170 °C for 2 h.

equivalent and increasing contents of Mg^{2+} or Ca^{2+} favours the further thermal stability of the corresponding precursors.

The crystallization of the amorphous phases takes place immediately after the full structural collapse of the precursors. The (Li)-A sample containing some undesired Na content, as occluded $NaAlO_2$ in its structural cages, crystallizes into β-eucryptite ($LiAlSiO_4$) and a small amount of nepheline ($NaAlSiO_4$).

Despite the full crystallization of all the samples, i.e. the absence of a residual amorphous phase, an extensive formation of microcracks has been detected especially for the sintered (Li)-A sample. Such behaviour has been mainly attributed to the high thermal expansion anisotropy of β-eucryptite. In this case, in contrast with the behaviour detected for glass-ceramics of the same composition, negligible microstresses are caused by the difference in the expansion coefficients at the interface between residual amorphous phase and crystallized phases.

The thermal crystallization of (Li–Ca)-A-based precursors gives, as the main phase, β-eucryptite of the poor silica variety, and then some anorthite $(Ca,Na)Al_2Si_2O_8$. The microcracks detected are less frequent in comparison with those observed for the corresponding (Li)-A sample.

The behaviour of the (Li–Mg)-A series to thermal crystallization differs from the previous zeolitic precursors. The β-eucryptite-like phases that crystallized at intermediate temperatures contain Mg which is exsoluted at the higher temperatures of thermal treatment giving place to $MgO{\cdot}Al_2O_3$ spinel. The content of this secondary phase increases with the increase of Mg content of the starting precursor so favouring the formation of β-eucryptite-like phases richer in SiO_2. The latter phases, characterized by a lower thermal expansion anisotropy than that of β-eucryptite, explain the presence of rare microcracks in products sintered from the (Li–Mg)-A precursors.

Acknowledgements

This work was carried out with the financial contribution of the Ministry of University and Scientific and Technological Research, bando: COFIN 2000, protocollo: MM09071425.

References

1. Pillars, W. W. and Peacor, D. R., Crystal structure of beta eucryptite as a function of temperature. *Am. Mineral*., 1973, **58**, 681–690.
2. Hatch, R. A., System $Li_2O{\cdot}Al_2O_3{\cdot}2SiO_2$ (eucryptite)-SiO_2; High temperature part of diagram. *Am. Mineral*., 1943, **28**, 471–496.
3. Roy, R., Roy, D. M. and Osborn, E. F., Compositional and stability relationship among the lithium aluminosilicates: eucryptite, spodumene, and petalite. *J. Am. Ceram. Soc*., 1950, **33**(5), 156–161.
4. Lynch, J. F., Ruderer, C. G. and Duckworth, W. H., *Engineering Properties of Selected Ceramic Materials*. The American Ceramic Society, Columbus, Ohio, 1966.
5. Hummel, F. A., Thermal expansion of some synthetic lithia minerals. *J. Am. Ceram. Soc*., 1951, **34**(8), 235–239.
6. Gillery, F. H. and Bush, E. A., Thermal contraction of β-eucryptite ($Li_2O.Al_2O_3.2SiO_2$) by X-ray and dilatometer methods. *J. Am. Ceram. Soc*., 1959, **42**(4), 175–177.
7. Hummel, F.A., US Pat. No. 2785080, 12 March, 1957. Reissue No. 24795, 15 March, 1960.
8. Schultz, H., Thermal expansion of beta-eucryptite. *J. Am. Ceram. Soc*., 1974, **57**(7), 313–318.
9. Behruzi, M. and Hahn, T. H., High lithium aluminium silicate and related phases in the lithium aluminium silicate-lithium gallium silicate-lithium aluminium germanate-lithium gallium germanate system. *Z. Kristallogr., Kristallgeometrie, Kristallphys., Kristallchem*., 1971, **133**, 405–421.
10. Scheidler, H. and Rodek, E., Li_2O–Al_2O_3–SiO_2 glass-ceramics. *Am. Ceram. Soc. Bull*., 1989, **68**(11), 1926–1930.
11. Subramanian, M. A., Corbin, D. R. and Chowdhry, U., Zeolites as precursors to alminosilicate-based ceramics for microelectronic packaging. *Adv. Ceram*., 1989, **26**, 239–247.
12. Corbin, D. R., Parise, J. B., Chowdhry, U. and Subramanian, M. A., Designing zeolites as novel precursors to electronic ceramics. *Mater. Res. Soc. Symp. Proc*., 1991, **233**, 213–217.
13. Parise, J. B., Corbin, D. R. and Subramanian, M. A., The role of strontium in the densification of Sr-zeolite-A to the low dielectric ceramic, anorthite. *Mater. Res. Bull*., 1989, **24**, 303–310.
14. Subramanian, M. A., Corbin, D. R. and Chowdhry, U., Better ceramic substrates through zeolites. *Bull. Mater. Sci*., 1993, **16**, 666–678.
15. Hoghooghi, J., Mckittrick, C., Butler, C. and Desch, P., Synthesis of celsian ceramics from zeolite precursors. *J. Non-Cryst. Solids Lett*., 1994, **38**(2), 175–180.
16. Mckittrick, J., Hoghooghi, B. and Lopez, O. A., Vitrification and crystallization of barium aluminosilicate glass ceramics from zeolite precursors. *J. Non-Cryst. Solids*, 1996, **197**, 170–178.
17. Hoghooghi, B., Mckittrick, J., Helsel, E. and Lopez, O. A., Microstructural development, densification, and hot pressing of celsian ceramics from ion-exchanged zeolite precursors. *J. Am. Ceram. Soc*., 1998, **81**(4), 845–852.
18. Dell'Agli, G., Ferone, C., Mascolo, M. C. and Pansini, M., Thermal transformation of Ba-exchanged A and X zeolites into monoclinic celsian. *Solid State Ionics*, 2000, **127**, 309–317.
19. Dondur, V. and Dimitrijevic, R, The thermal transformation of sodium lithium A zeolites. A new polymorph of lithium aluminium silicate ($LiAlSiO_4$). *J. Solid State Chem*., 1986, **63**, 46–51.
20. Norby, P., Thermal transformation of zeolite Li-A(BW): the crystal structure of γ-eucryptite, a polymorph of lithium aluminium silicate $LiAlSiO_4$. *Zeolites*, 1990, **10**(3), 193–199.
21. Powder Diffraction File Card No 26-839, JPCDS, Swarthmore, PA, 1995.
22. Powder Diffraction File Card No 47-27, JPCDS, Swarthmore, PA, 1995.
23. Powder Diffraction File Card No 35-424, JPCDS, Swarthmore, PA, 1995.
24. Ray, S. and Muchow, G. M., High-quartz solid solution phases from thermally crystallized glasses of compositions (Li_2O,MgO).Al_2O_3.nSiO_2. *J. Am. Ceram. Soc*., 1968, **51**(12), 678–682.
25. Powder Diffraction File Card No 41-1486, JPCDS, Swarthmore, PA, 1995.
26. Kingery, W. D., Bowen, H. K. and Uhlmann, D. R., *Introduction to Ceramics*, 2nd Edn. John Wiley & Sons, New York, 1976, p. 135.
27. Colantuono, A., Dal Vecchio, S., Mascolo, G. and Pansini, M., Thermal shrinkage of various cation forms of zeolite, A.. *Thermochimica Acta*, 1997, **296**, 59–66.